Journal of Colloid and Interface Science 579 (2020) 258–268

Contents lists available at ScienceDirect

Journal of Colloid and Interface Science

journal homepage: www.elsevier.com/locate/jcis

Modification of pyrogenic carbons for phosphate sorption through binding of a cationic polymer

Zhengyang Wang [a,1], Santanu Bakshi [a,1,2], Chongyang Li [b,3], Sanjai J. Parikh [b], Hsin-Se Hsieh [a,4], Joseph J. Pignatello [a,*]

[a] Department of Environmental Sciences, The Connecticut Agricultural Experiment Station, New Haven, CT 06504, USA
[b] Department of Land, Air and Water Resources, University of California, Davis, CA 95616, USA

HIGHLIGHTS

- Sorption density of PO_4-P on GAC and biochars is improved after pDADMAC coating.
- Polymer coverage was confirmed by imaging and spectroscopic analyses.
- Sorption mechanism on pDADMAC-coated and reference Mg-doped biochars was elucidated.
- Sorption was partly inhibited by sulfate, carbonate, and manure extracts.
- Sorption was more reversible with pDADMAC-coated than Mg-doped biochars.

GRAPHICAL ABSTRACT

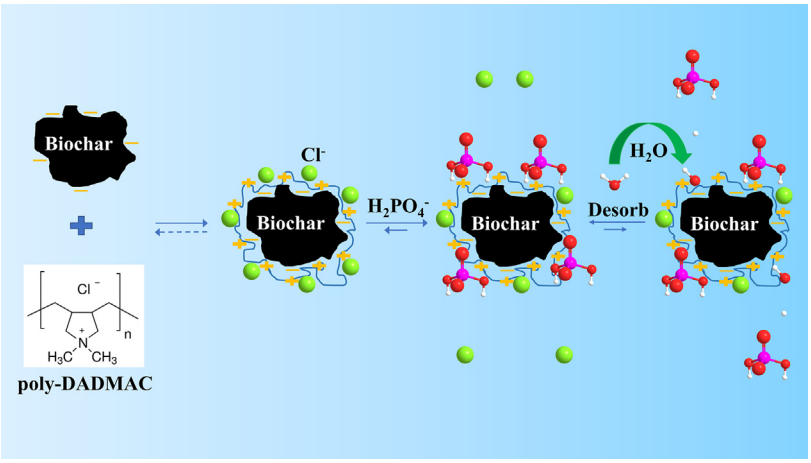

ARTICLE INFO

Article history:
Received 19 March 2020
Revised 29 May 2020
Accepted 10 June 2020
Available online 14 June 2020

Keywords:
Modified biochar
Phosphate sorption
Competitive sorption
Phosphate recycling
Animal waste

ABSTRACT

This study reports on the development of modified pyrogenic carbonaceous materials (PCMs) for recovering orthophosphate (PO_4-P). The PCMs include softwood and hardwood biochars and a commercial granular activated carbon (GAC) that were modified by irreversible adsorption of the quaternary ammonium polymer, poly(diallyldimethylammonium) chloride (pDADMAC), which reverses electrokinetic charge and increases PO_4-P sorption. MgO-doped biochars were prepared by a literature method for comparison. Imaging and spectroscopic analyses characterize pDADMAC coverage, MgO doping, and binding of PO_4-P. At environmentally relevant concentrations, PO_4-P sorption by the pDADMAC-treated biochars was ~100 times greater than that of the corresponding unmodified biochars, and was comparable to that of the corresponding MgO-doped biochars on a coating content basis. The pDADMAC-coated carbons bind PO_4-P by ion exchange, while the MgO-doped biochars bind PO_4-P principally by forming an amorphous Mg phosphate species. Susceptibility to competition from other relevant anions (Cl^-, NO_3^-, HCO_3^-/CO_3^{2-}, SO_4^{2-}) and poultry and dairy manure extracts was moderate and comparable for the two types of modified softwood biochars. Sorption to the pDADMAC-treated biochars appears to be more reversible than to the

* Corresponding author.
E-mail address: Joseph.Pignatello@ct.gov (J.J. Pignatello).
[1] S. Bakshi and Z. Wang contributed equally to this work.
[2] Present address: Bioeconomy Institute, Iowa State University, Ames, IA 50011, USA.
[3] Present address: Department of Crop Sciences, University of Illinois, Urbana-Champaign, Urbana, IL 61801, USA.
[4] Present address: Bureau of Environmental Inspection, Environmental Protection Administration, R.O.C., 497 Section 2, Liming Road, Taichung City 40873, Taiwan.

https://doi.org/10.1016/j.jcis.2020.06.054

MgO-doped biochars using stepwise water extraction. Greater reversibility may be advantageous for trapping and recycling phosphate.

1. Introduction

Nutrient pollution can cause water quality degradation and ecosystem disruption, resulting in hypoxia, eutrophication, harmful algal blooms, and economic impacts due to loss of commercial and recreational value of water bodies [1,2]. The predominant sources of nitrogen (N) and phosphorus (P) include animal feeding operations, fertilizer and manure application to agricultural fields, non-point source runoff, and effluents from wastewater treatment plants [3,4]. P is often the limiting nutrient. Cost-effective engineering techniques are urgently needed in agriculture to remove excess nutrients from animal wastes, to minimize or mitigate nutrient runoff, and to recycle nutrients back to the land to achieve sustainable food production while protecting the environment. Viable recycling strategies for N and P in organic wastes to date are sparse [5–7].

This study represents a novel strategy for trapping excess phosphate based on the use of modified pyrogenic carbonaceous materials (PCMs). The target nutrient of the present study is orthophosphate (PO_4-P), and the PCMs tested include biochars derived from biomass wastes and a commercial granular activated carbon (GAC). The modified PCM could be used for sequestering nutrients in composted animal wastes, as barriers in treatment of wetlands, or as bed adsorbents in other water treatment systems. It is envisioned that the captured nutrients would be recyclable, either through their direct recovery from the spent PCM, or by returning the spent PCM to the soil to serve as a slow-release source of fertilizer. Thus, it is highly desirable for the trapped nutrients to be present in reversibly-bound forms that are less leachable but still bioavailable to crop plants. Biochars derived from agricultural and forestry wastes have received considerable attention as soil amendments [8] with potentially beneficial functions, including carbon sequestration and storage [8–11], liming effects, increased cation exchange capacity, improved water holding capacity [12], and reduced mobility and bioavailability of chemical contaminants [13–19], favorable effects on microbial communities, and mitigation of greenhouse gas emissions [20,21]. Hence, designed nutrient retention capability would provide added value to the biochars.

As-produced biochars, however, are not reliable as specific adsorbents of common nutrients. While they can bind ammonium due to their modest cation exchange capacity [22,23], their anion exchange capacity (AEC) is ordinarily low [24] and thus their ability to bind phosphate and nitrate [22,23,25–28] is unimpressive and poorly predictable from feedstock properties [29]. Nevertheless, some studies suggest that biochar amendment can enhance nutrient bioavailability and plant uptake in soil [e.g., 22,28,30,31–35], but the literature is decidedly mixed on this subject, and the mechanisms by which biochar retains nutrients are poorly understood.

We sought ways to increase the binding capacity of biochars for anionic nutrients. In the present study we focused specifically on PO_4-P, which exists predominantly as $H_2PO_4^-$ and HPO_4^{2-} ions (pK_a, 2.1, 7.2, 12.4) at typical pH of soil and composts. Our approach for enhancing PO_4-P binding was to reverse the charge on the adsorbent by noncovalently, but irreversibly, binding a cationic polymer, poly(diallyldimethylammonium) chloride (pDADMAC), a strategy originally proposed by Hsieh and Pignatello for activated carbons in another context [36]. pDADMAC is used commercially in the wastewater- and drinking water-treatment industries for flocculating small particles, algae, bacteria, viruses, microbes, and dissolved organic matter (DOM), where it is generally regarded as safe [37]. Recently, pDADMAC coated on clay was proposed for use in urban stormwater remediation [38] and pDADMAC in layer-by layer coatings on membranes for use in phosphoric acid recovery at low pH [39].

Other strategies for modification of biochars and other sorbents for the purpose of retaining nutrients have been investigated. In a review, Kumar et al. [3] concluded that adsorption can achieve very low concentrations of PO_4-P, and offers the possibility to recover the P by regeneration of the adsorbent. After reviewing P adsorbents, Rittmann et al. [40] concluded that binding to Mg-based solids, Ca-based solids, Fe-based solids, and phosphate-selective ion exchangers are the most promising. Biochars produced from tomato plants enriched with Mg via natural uptake from fortified soil [41], or biochars made from biomass wastes pre-soaked in $MgCl_2$ solution [42] yielded products with deposited or incorporated Mg minerals. These Mg-modified biochars were effective at sorbing PO_4-P. While sorption reversibility was not specifically addressed in those studies, PO_4-P sorbed by the tomato biochars was evidently bioavailable.

In this study we hypothesized that pDADMAC coating of biochars and GAC could result in a material that could effectively adsorb PO_4-P. We intended to explore the potential concept and mechanism of PO_4-P attachment with this cationic polymer-coated biochar under conditions relevant to our proposed applications in animal wastes management. In view of the results mentioned above with MgO-doped biochars, we compared pDADMAC-treated and MgO-doped biochars for PO_4-P retention.

2. Materials and methods

2.1. Materials and materials preparation

Biochars were produced from softwood and maple wood shavings via slow pyrolysis process. The softwood shavings were purchased from Agway (packaged by Empaquetages Messier, Quebec, Canada; species unspecified by the packager). The maple shavings originated from lumber purchased from a local store. The shavings were washed with water and allowed to dry at 65 °C for 72 h in a conventional oven. The shavings were then placed in a stainless-steel pan in the center of a sealed temperature-programmable furnace (GCF1700, Across International, NJ). A flow of N_2 at 4 L/min was maintained for 30 min to create an anoxic condition, and then reduced to 1.5 L/min of N_2 during pyrolysis. The furnace was heated to 100 °C for 1 h to remove moisture and then at 20 °C/min to 500 °C where it was held for 2 h as the residence time. After the furnace was allowed to cool overnight to ~100 °C, the biochar product was removed and misted with water to prevent spontaneous combustion in air. The product was stored in air at room temperature for at least 2 weeks to dry and complete chemisorption of oxygen. The product was then gently crushed to pass through a 0.5 mm mesh sieve. Carboxylic acid groups of softwood and maple wood biochars were quantified via the modified Boehm titration method [43], and the contents were determined to be 0.29 and 0.22 mmol/g, respectively.

Norit RO GAC (325 mesh) was obtained from Calgon Carbon (Moon Township, PA). pDADMAC (average molecular weight 200,000–350,000, 20% aqueous solution) was purchased from Sigma-Aldrich. Other reagents were purchased from Sigma-Aldrich or Fisher Scientific. Water (18.2 MΩ·cm) used in this study was tap water purified in a Milli-Q Integral 10 system. Manures were obtained from a local farm near Davis, California. Freshly-collected dairy or poultry manures (300 g wet weight) were extracted with 1.5 L of 18.2 MΩ·cm water for 12 h in a 2-L bottle on a shaker. After settling, the supernatant liquid phase was transferred to a 50-mL tube and centrifuged at 5,858 RCF for 15 min. The clarified liquid was then filtered through a 0.45 μm cellulose acetate membrane using a vacuum apparatus. Filtered liquids were frozen at −80 °C and freeze-dried to obtain the solid form of the water-soluble manure substance. Solids were stored in amber vials at 4 °C.

2.2. Modification of the carbonaceous materials

Treatment of biochars with pDADMAC was carried out by a method similar to the one used for the GAC [36]. Biochar (5 g) was mixed with as-purchased pDADMAC solution (4 or 16 g) and water (16 mL) in a 60-mL glass vial and equilibrated for 24 h on an end-over-end rotating shaker at room temperature. After equilibration, the mixture was separated in a swing-bucket centrifuge at 2369 RCF for 30 min and the supernatant liquid removed for pDADMAC analysis. To remove non- and loosely-bound pDADMAC the centrifugate was washed with several 50-mL portions of water for 30 min each, followed each time by centrifugation and decantation of the supernatant until the pDADMAC concentration in the final washing was below method detection limit. pDADMAC concentration was determined by a reported method [36]. An account of the pDADMAC amount in each washing step for the softwood biochar is shown in Fig. S1 of the Supplementary Material.

After the final washing, the collected solid was dried in an oven at 65 °C for 72 h. The treated biochars will be referred to hereafter as low- or high-pDADMAC softwood or maple biochars, respectively, based on the nominal pDADMAC amount (4 or 16 g pDADMAC solution) used in their preparation. The actual adsorbed pDADMAC concentrations in the biochars were calculated based on the difference in elemental N contents relative to the corresponding unmodified biochar (Table S1) to be 15.0 and 23.1 mg/g for the low- and high-pDADMAC softwood biochars, respectively, and 23.1 and 30.0 mg/g for the low- and high-pDADMAC maple biochars, respectively. The GAC contained 102 mg/g pDADMAC [36]. Control samples of biochar and GAC were prepared in the same way except without pDADMAC.

The MgO-doped biochars were prepared as follows. Shavings (50 g) were mixed with aqueous magnesium acetate solution (200 mL) at different concentrations in Nalgene (high-density polyethylene) bottles. The magnesium acetate concentration in the water of each bottle was adjusted to achieve a final nominal elemental Mg content of the biochar product to be 3%, 5%, 10%, or 20% Mg by weight, assuming an 80% loss of the initial biomass due to pyrolysis. The bottles were shaken for 24 h in a reciprocal shaker at room temperature and then the content of each bottle was brought to dryness in a conventional oven at 65 °C for 72 h. The resulting material was transferred to a stainless-steel pan and pyrolyzed at 500 °C under nitrogen in the manner described above. These products are referred to throughout as 3%, 5%, 10%, or 20% Mg softwood or maple biochars, respectively, based on their nominal Mg content. The actual Mg contents were 1.31%, 2.51%, 3.88%, or 7.30% for Mg-doped softwood biochars, and 1.52%, 2.78%, 5.02%, and 7.20% for Mg-doped maple biochars (for details see Text S1). A control biochar in each case was carried through the same procedure but without the Mg salt; the controls had about 0.1% natural Mg (Table S1).

2.3. Materials characterization

The GAC and pDADMAC-treated GAC were characterized previously [36]. The C, H, N, Si, P, total metals, and soluble metals contents of the biochars were determined as described in Text S1 and are reported in Table S1. Characterizations of dairy and poultry manure extracts are seen in Text S2 and characteristics in Table S2.

Morphology and structure of biochars were observed at different magnifications with a scanning electron microscope (SEM, SU8230, Hitachi) and a transmission electron microscope (TEM, HT7800, Hitachi). Mg and N distributions on biochars were mapped with an energy dispersive X-ray spectrometer (EDS, XFlash 5060FQ, Bruker) and wavelength-dispersive spectrometer (WDS, JXA-8530F, JEOL), respectively. Ca element mapping was scanned via WDS for the vestigial cell wall structure of the softwood, exposed by polishing the biochar embedded in epoxy resin. The Mg crystallinity was identified using a Rigaku SmartLab X-ray diffractometer (XRD instrument) with a Cu Kα radiation source. Surface chemical composition before and after PO_4-P sorption on freeze-dried samples was analyzed by X-ray photoelectron spectroscopy (XPS, VersaProbe II, PHI) with Al Kα radiation; photoelectron binding energies were referenced to C1s peak at 284.8 eV [44]. Electrokinetic (zeta) potentials were measured on a Malvern Zetasizer (Nano-ZS90). At a solid: water ratio of 20 mg: 50 mL, the suspension was vigorously shaken by hand before 10 mL aliquots were dispensed into 22-mL high-density polyethylene (HDPE) screw-cap vials. Then, the pH of the aliquots was adjusted to a desired value by adding HCl or NaOH and then allowed to equilibrate for 12 h. The pH was then measured again just before two zeta potential measurements on each of the two 1-mL subsamples. Carbon dioxide porosimetry at 0 °C was conducted using an Autosorb iQ (Anton Paar) to compute specific surface area and pore size distribution using built-in software.

2.4. Sorption and desorption isotherms

Sorption isotherms were constructed by placing solid (0.1 g) and water (20 mL) in a 22-mL HDPE screw-cap vial. The pH of the mixture was adjusted to 8.0 with either dilute HCl or NaOH and allowed to hydrate for 24 h. The pH was readjusted to 8.0 and then an appropriate small volume of PO_4-P stock solution (1000 mg PO_4/L as KH_2PO_4 adjusted to pH 8.0 with NaOH) was added to achieve a desired initial concentration, and the vials were placed on the end-over-end rotating shaker at 30 rpm for 72 h at 20 ± 2 °C. Afterward, the contents were filtered through a 0.45 μm Teflon membrane to obtain a clear filtrate for analysis. The final pH was 8.1–8.2 for the unmodified biochars, 7.6–7.8 for the pDADMAC-biochars, and 9.0–10.6 for the Mg-doped biochars. The concentration of PO_4-P remaining in solution after 72-h sorption in samples to which no PO_4-P had been added was below the method detection limit in all cases.

Sorption of PO_4-P at each datum was calculated by:

$$q = \frac{m_{\text{added}} - C_{\text{aq}} V_{\text{aq}}}{M_{\text{carbon}}} \quad (1)$$

where q is the sorbed concentration (mg PO_4/kg), m_{added} the mass as PO_4 (mg) added, C_{aq} the concentration in solution after sorption (mg PO_4/L), V_{aq} the liquid phase volume (L), and M_{carbon} the mass (kg) of biochar or GAC. Data showing <15% sorption of PO_4-P_{added} were rejected.

Values of the distribution ratio K_D (L/kg) at 10 mg/L and 100 mg/L phosphate calculated on interpolation of the Freundlich fits are listed in Table S3:

$$K_D = \frac{q}{C_{aq}} = K_F C_{aq}^{n-1} \quad (2)$$

where K_F and n are the Freundlich affinity-capacity and linearity parameters, respectively.

For desorption, the phosphate-loaded biochars after 72 h of sorption were separated from their supernatant liquid by vacuum filtration through a 0.45 μm membrane, and the biochar together with the membrane was quantitatively transferred back to the same vial. Then, 20 mL of 18.2 MΩ•cm water was added, the pH readjusted if necessary to 8.0, and the vials shaken for a 72 h desorption period. The desorption process was repeated two more times for the pDADMAC-treated biochars. The supernatants collected from desorption steps were each filtered through a 0.45 μm membrane syringe filter prior to PO_4-P analysis.

Dissolved PO_4-P concentration was measured colorimetrically at 880 nm by the ascorbic acid method [45–47] using a mixed reagent consisting of sulfuric acid (2.5 M), ammonium molybdate (0.033 M), antimony potassium tartrate (0.009 M) and ascorbic acid (0.1 M). pDADMAC concentration was ensured to be below 20 mg/L (as solid), where it begins to interfere with color development.

2.5. Inhibition by natural ions

Phosphate adsorption experiments for the biochars were conducted in duplicate at 20 °C in the presence of environmental-relevant anions or manure extracts. Biochar (5 mg) was added to 10 mL water in a 22-mL HDPE screw-cap vial, the pH adjusted to 8.0, and the vials mixed on the end-over-end rotating shaker at 50 rpm for 24 h. Meanwhile, stock solution of phosphate, test anions (Cl^-, NO_3^-, HCO_3^-/CO_3^{2-}, or SO_4^{2-}; K salts), and pre-filtered manure extracts were prepared and adjusted to pH 8. After pre-equilibration of solids with water, phosphate stock solution and either test anion or manure extract stock solution were added in quick succession. The initial concentrations in each vial were 1.02 mM PO_4-P, 2 mM anion, or enough manure extract to give 20.3 mg/L of dairy or 18.0 mg/L of poultry, based on dissolved organic carbon content. The control had 1.02 mM PO_4-P only. The pH was then re-adjusted to 8.0 and the samples mixed for 72 h. The final pH was recorded (Fig. S2). A portion of the liquid phase was filtered (0.45 μm membrane) and analyzed for PO_4-P concentration. Since the dairy and poultry manures have natural phosphate (2.67% and 0.20% of PO_4-P on dry mass basis) and the added competitor affects phosphate partitioning between the solid and liquid phases, the effects on sorption were interpreted in terms of the effects on the phosphate distribution ratio (K_D).

3. Results and discussion

3.1. Adsorbent characteristics

Elemental contents of C, H, N, Si, P, and metals were similar for the unmodified maple and softwood biochars (Table S1). Small amounts of native Ca, K, Mg, and Na of both biochars were water soluble, but no PO_4-P was detected in the water extracts, so if native P (196 and 241 mg P/kg for maple and softwood, respectively) contained any PO_4-P, it was assumed not to participate in PO_4-P sorption during construction of the isotherms. The N content of the biochars increased with the level of pDADMAC treatment. These changes were used to calculate pDADMAC contents.

Carbon dioxide adsorption on the unmodified, high-pDADMAC, and 20% Mg softwood biochars is highly reversible (Fig. S3). The specific surface areas (and pore volumes) calculated from the CO_2 isotherms of unmodified, high-pDADMAC, and 20% Mg-doped softwood biochars are 579 (0.158), 571 (0.152), and 509 m^2/g (0.121 cm^3/g), respectively. Since pDADMAC did not change the specific surface area and micropore size distribution relative to the unmodified biochar, pDADMAC does not significantly block micropores, and MgO has only slight effect. The specific surface area and pore volume for the unmodified maple biochar are 560 m^2/g and 0.144 cm^3/g, respectively, close to those values for the unmodified softwood biochar.

For imaging and spectroscopic analyses, we focused on the unmodified and modified softwood biochars. The SEM images clearly show the honeycomb-like structure of the vestigial cell wall for unmodified (Figs. S4a-b) and high-pDADMAC (Fig. 1a-b) softwood biochars. The SEM-WDS images reveal 10–20 μm macropores with exposed vestigial cell walls semi-normal to the sample surface (Figs. S4c-d and Fig. 1c-d). While there is background N from the unmodified biochar (Fig. S4e), the intensity of N in the pDADMAC-coated sample can be seen to be enhanced along the wall structure (Fig. 1e) which indicates that the polymer was sorbed along the walls and even further into the macropores.

The TEM images of high-pDADMAC softwood biochar (Fig. 1h-i) show a "fluffy" structure at the edge of the grain, likely due to polymer attachment to the surface as we have proposed. These structures are not observed on the unmodified (Fig. 1f) nor the 20% Mg (Fig. 1g) biochars. The N1s XPS spectra show a peak centered at 402.8 eV which corresponds to quaternary ammonium N [48–50] (Fig. 2a) detected only after pDADMAC treatment, supporting the TEM observations and elevated elemental N content.

The XRD spectrum of 20% Mg-doped softwood biochar shows the presence of periclase (MgO) (Fig. S5a). The Mg2p XPS spectrum shows a peak consistent with only the presence of MgO (Fig. 2c). The SEM image along with Mg elemental mapping are shown in Fig. S6. Although possible that MgO would take up CO_2 from ambient air, no evidence for $MgCO_3$ appeared in the XRD or Mg2p XPS spectrum, indicating that this species could be present in only small concentration at best. The high reversibility of CO_2 adsorption on the 20% Mg biochar (Fig. S3c) is indicative of a physisorption rather than a chemisorption process. Mg-doping slightly reduced the surface area and micropore volume (by 12% and 23%, respectively) at the highest level of doping. This caused a modest reduction in porosity larger than 0.7 nm, and a modest increase in porosity smaller than 0.4 nm (Fig. S3) compared to the unmodified biochar. Taken together, the evidence suggests a hierarchical pore structure of softwood biochars consisting of both macropores (Fig. 1) and micropores (Fig. S3). This hierarchical structure favors accessibility to micropores where most of the surface area, hence sorption sites, are located.

3.2. Zeta potential

Fig. 3 shows the zeta potentials of high pDADMAC-coated and 20% Mg-doped biochars at pH values bracketing the range used in the PO_4-P adsorption experiments for isotherms (to be discussed later). It reveals that the zeta potential of the maple and softwood biochars increased from negative to positive values after coating with pDADMAC. pDADMAC coating also reversed the charge of the GAC over a wide range of pH [36]. These results clearly show that surface modification of PCMs with pDADMAC introduces positive charge in excess of the surface negative charge carried by the carboxyl and hydroxyl groups that presumably serve as binding sites. By contrast, Mg doping does not reverse the charge (Fig. 3) and the biochar remains negatively charged over the range 9.6–10.8. The point of zero charge (pH_{pzc}) of nano-periclase (MgO) is reported to be 11.26 [51]. This means that the MgO associated with the Mg-doped biochars does not have the same surface acid-base character as nano-periclase.

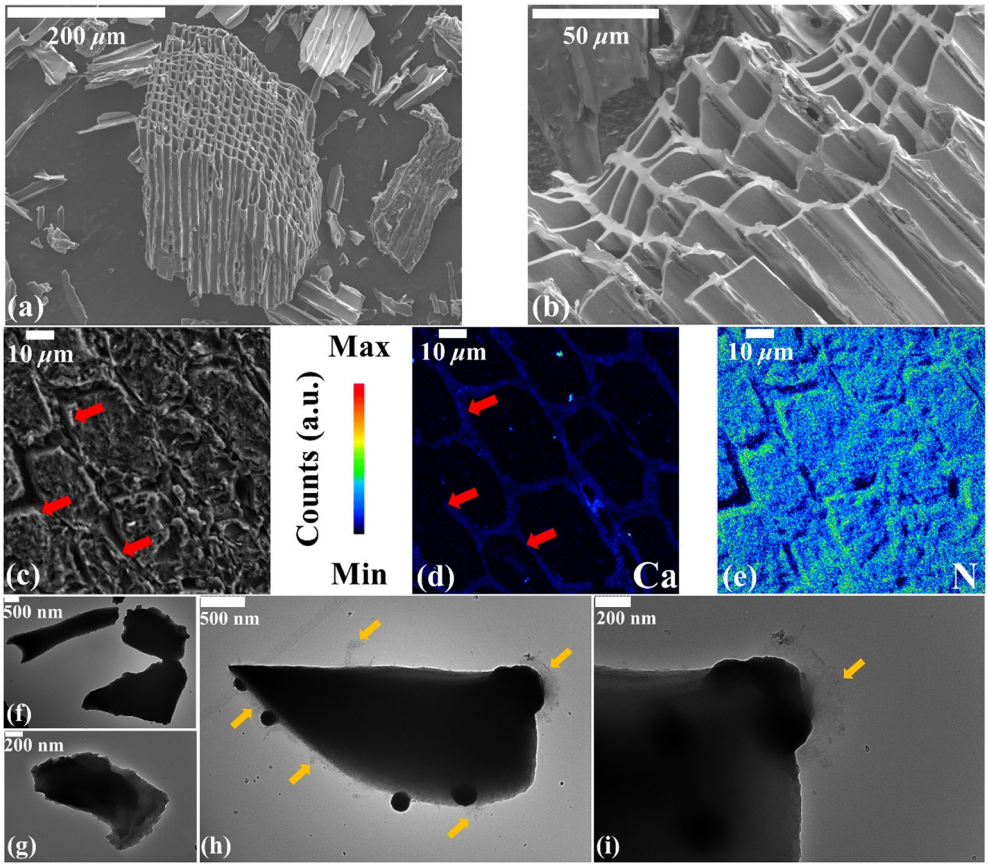

Fig. 1. SEM images of high-pDADMAC softwood biochar grains showing: (a) the cross section with the vestigial cell wall structure; (b) the vestigial cell wall structure at a higher magnification; (c) The exposed wall structure (the steeper (lighter) area approximately normal to the sample surface, indicated by the red arrows) of a single grain with WDS element mappings of (d) Ca and (e) N, respectively. Ca mapping reveals the vestigial cell wall structure and N mapping displays nitrogen distribution with the high-intensity signals on and around the wall areas. Note that different grains are imaged for (a)-(c). TEM images of (f) unmodified softwood biochar; (g) 20% Mg softwood biochar; and (h) and (i) high-pDADMAC softwood biochar at different magnifications. The yellow arrows denote the fluffy structure of the pDADMAC coating.

3.3. Phosphate sorption-desorption isotherms

The isotherms of PO_4-P at initial pH 8 on the pDADMAC-treated GAC compared to the as-received GAC are shown in Fig. 4. Treatment of the GAC with pDADMAC increased its affinity for PO_4-P by more than an order of magnitude at dissolved PO_4-P concentrations below ~10 mg/L. Sorption isotherms of PO_4-P for pDADMAC-treated and Mg-doped biochars at initial pH 8 are shown in Fig. 5. Unmodified maple biochar bound more PO_4-P than unmodified softwood biochar, even though the softwood biochar contained higher overall levels of polyvalent metal ions. Sorption of PO_4-P to the pDADMAC-treated series of biochars (Fig. 5a-b) increased with pDADMAC loading. The affinity of PO_4-P for the pDADMAC-treated maple and softwood biochars was similar. At dilute levels of dissolved PO_4-P (<30 mg/L), the high-pDADMAC biochars sorbed about 24–105 times more PO_4-P than the controls. The fits to the log-transformed Freundlich equation had regression coefficients R^2 ranging from 0.864 to 0.987, but it can be seen in Fig. 5 that in some cases the data followed a curve rather than a straight line.

Sorption of PO_4-P to the Mg-doped biochars (Fig. 5c-d) was related to the Mg content. At levels of dissolved PO_4-P below 30 mg/L, the 20% Mg biochars sorbed approximately 48–105 times more PO_4-P than the controls. Separate experiments showed that addition of phosphate to water extracts of the 20% Mg-doped biochars at pH 8 did not induce turbidity or show evidence of precipitation. This observation rules out the possibility that PO_4-P removal from solution was caused by independent coagulation of magnesium phosphates originating from solubilization of Mg^{2+} from the solid into the bulk solution. Sorption of PO_4-P to the 20% Mg softwood and maple biochars are lower than PO_4-P sorption to a Mg-doped biochar made from $MgCl_2$-impregnated sugar beet tailings [42] over a similar range in solution concentration. The difference in sorption can be explained by the difference in Mg content (7.20% and 7.30% Mg for the maple- and softwood-derived biochars, respectively, vs. 26% for the product made by Zhang et al. [42]). The 20% Mg-doped biochars are more effective adsorbents than the high-pDADMAC-coated biochars on a bulk mass basis, but it should be noted that the solution pH is higher in contact with the Mg-doped biochars, affecting phosphate speciation and sorption (see Section 3.4). If we compare sorption on a mass basis of the coating content, we find that sorption to high-pDADMAC-coated biochars is comparable to that of the 20% Mg-doped biochars (see Table S4). For example, at 10 mg/L dissolved PO_4-P, adsorption on high-pDADMAC and MgO-doped maple biochars are 97.1 and 70.5 mg/g coating, respectively; for the softwood case, they are 89.0 and 83.6 mg/g coating, respectively. Overall, sorption of phosphate by maple and softwood biochars are quite similar for the treated samples. However, the untreated maple sorbs more phosphate than the untreated softwood biochar, for which we have no explanation at this time.

We next studied desorption using a batch decant-and-replace method with 18.2 MΩ·cm water as the diluent. The pDADMAC-coated biochars received a three-step desorption (Fig. 6), whereas the Mg-doped biochars received a one-step desorption (Fig. 7), from selected points on the sorption branch. These experiments show that PO_4-P sorption reversibility is generally limited. This

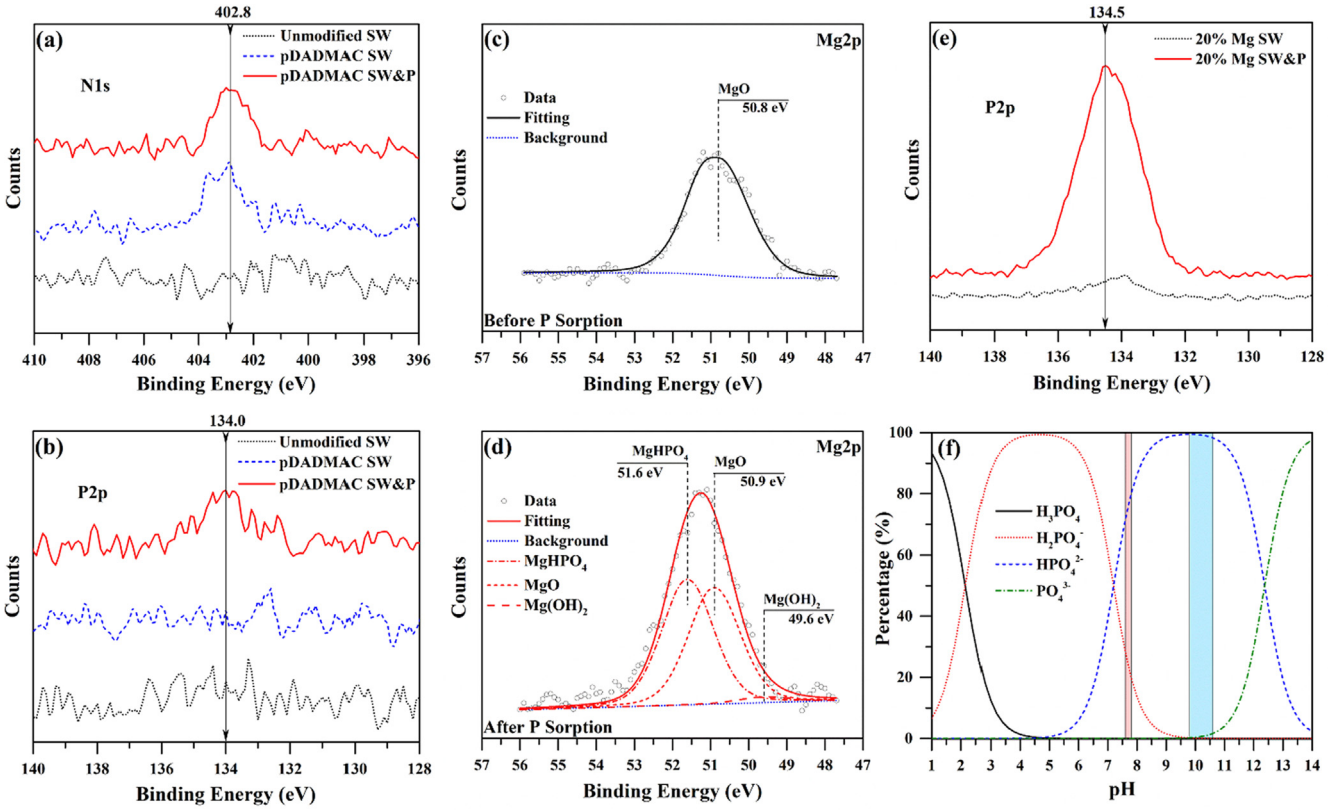

Fig. 2. XPS spectra for unmodified and high-pDADMAC-coated or 20% Mg-doped softwood (SW) biochars before or after phosphate (P) sorption at 300 mg $PO_{4\text{-}P}$/L initial concentration: (a) N1s and (b) P2p spectra for the pDADMAC series; and (c,d) Mg2p and (e) P2p for the 20% Mg doped series. Panel (f) shows PO_4-P speciation in water (MINTEQ v. 3.1): the red and blue shaded areas indicate the final pH ranges after phosphate adsorption by high-pDADMAC-coated and 20% Mg-doped biochars, respectively.

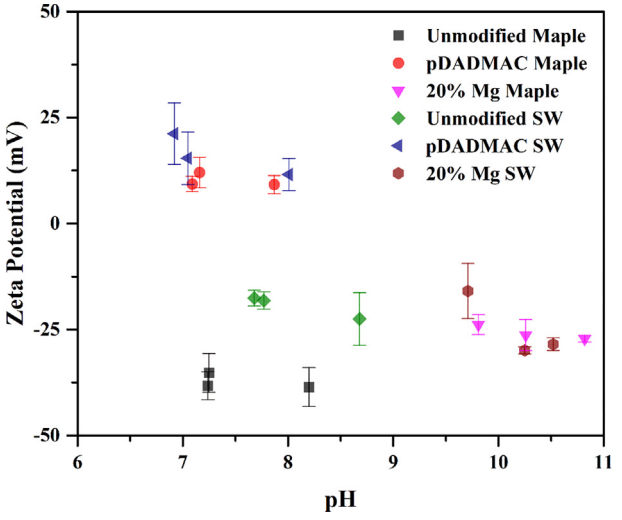

Fig. 3. Electrokinetic potential of unmodified, high-pDADMAC-coated, and 20% Mg-doped maple and softwood (SW) biochars. Phosphate not added. The pH ranges are selected according to the final pHs of the sorption experiments indicated in Fig. 2f. Error bars represent standard deviation (n = 4).

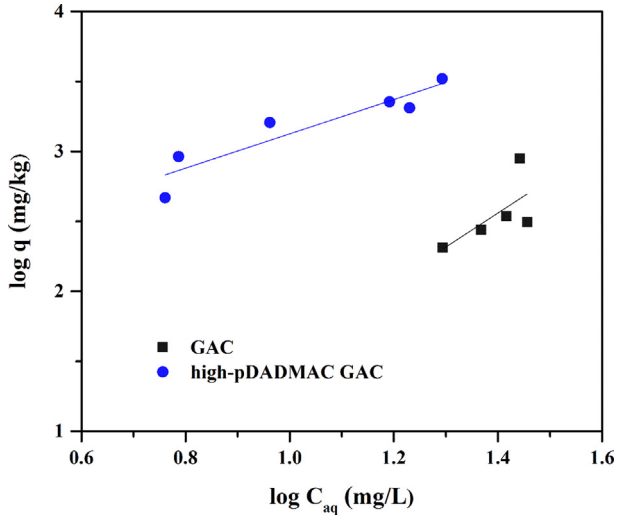

Fig. 4. Phosphate sorption by unmodified and high-pDADMAC-coated Norit RO granular activated carbon (GAC). Lines are best linear fit of the data to the log-transformed Freundlich equation.

could be due in part that the diluent lacks ions other than hydroxide which could displace the sorbed PO_4-P ions. Sorption is irreversible for the unmodified biochars (Fig. 6a and d, and Fig. 7a). For the pDADMAC-treated biochars, reversibility decreases with successive desorption steps, and increases with the level of pDADMAC treatment (e.g., compare Fig. 6c to Fig. 6b). For the Mg-doped biochars, reversibility is lowest for the biochar with the highest Mg content and generally lower than the pDADMAC-coated biochars.

3.4. Inhibition by natural ions and pH effects

Fig. 8a plots the distribution ratio K_D when phosphate is present alone or together with select inorganic ions (Cl^-, NO_3^-, HCO_3^-/CO_3^{2-}, or SO_4^{2-}) or dairy or poultry manure extracts. The addition of anions

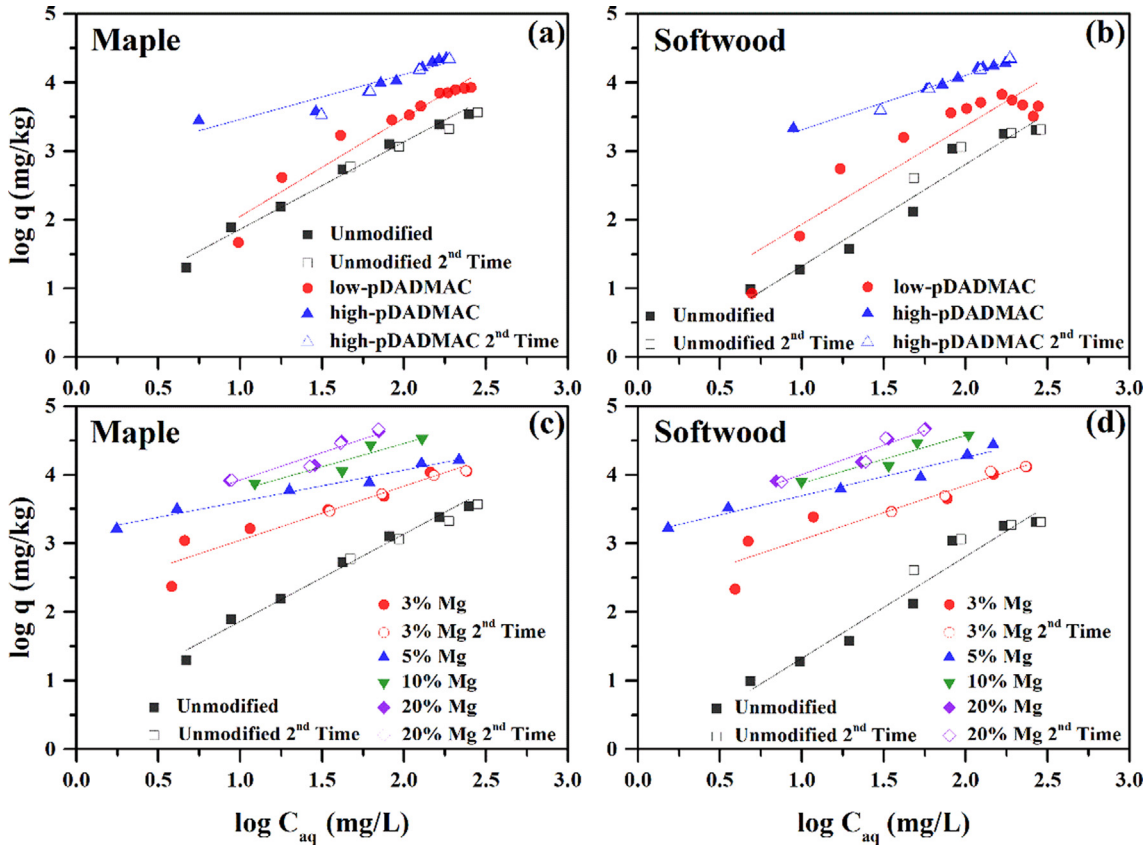

Fig. 5. Phosphate sorption isotherms on (a) unmodified and pDADMAC-coated maple biochars, (b) unmodified and pDADMAC-coated softwood biochars, (c) unmodified and Mg-doped maple biochars, and (d) unmodified and Mg-doped softwood biochars. C_{aq} is the liquid concentration and q the adsorption density. Second time means repeated experiment for selected systems. Lines are best linear fit of the data to the log-transformed Freundlich equation. See text for experimental conditions. The isotherms are reproducible as can be seen from the repeated experiments indicated in the graphs.

or manure extracts inhibits PO_4-P sorption on softwood biochars to different degrees. With phosphate alone, the order in K_D (L/kg) is high-pDADMAC (94.5) < 10% Mg (144) < 20% Mg (178), consistent with the trend seen in the isotherms (Fig. 5). Chloride and nitrate have negligible effect on phosphate sorption by pDADMAC-coated biochars, but slightly suppress phosphate sorption by the Mg-doped biochars. (Bi)carbonate and sulfate have more pronounced effects on sorption of phosphate by both pDADMAC-coated and Mg-doped biochars, decreasing the K_D by as much as half.

The inhibitory effect follows the same order for all four types of biochars: Cl^- < NO_3^- < HCO_3^-/CO_3^{2-} < SO_4^{2-}. For the pDADMAC-coated biochars, the trend is consistent with the chromatographic elution order of the respective ion on strong-base quaternary ammonium anion exchange resins, and can be explained classically in terms of Coulombic forces (monovalent vs. divalent ions) and van der Waals forces due to molecular size (35.5, 62.0, 61.0/60.0, and 96.1 g/mole, respectively) and polarizability [52]. According to this mechanism, PO_4-P should encounter minimal competition from chloride and nitrate but more significant competition from (bi)carbonate and sulfate.

The Mg-doped biochars may bind PO_4-P by forming a Mg phosphate species (see Section 3.5). It is likely that the such reaction would be disrupted more by sulfate and (bi)carbonate than chloride and nitrate. Xie et al. [53] reported SO_4^{2-} reduced PO_4-P sorption on Mg-doped diatomite more so than Cl^- and NO_3^-, ascribing it to the ability of sulfate to block surface sites and reduce surface charge density.

Dairy and poultry manure extracts inhibit PO_4-P sorption to a comparable extent as SO_4^{2-} at the concentrations tested. Table S2 reveals that the manure extracts contain, in addition to organic matter, native levels of Cl^-, NO_3^-, S (probably as SO_4^{2-}), and HCO_3^-/CO_3^{2-} (difference between total carbon and total organic carbon). In addition, Cooperband and Good [54] observed that poultry manure contains calcium and magnesium phosphate minerals. However, in our case, such phosphate precipitates in the manure would have been filtered out. It is not possible to attribute inhibition to any particular species in the extracts. Weyers et al. [55] found that manure extracts inhibit PO_4-P adsorption to synthesized calcite.

Fig. 8b shows the effects of pH. For high-pDADMAC softwood biochar, PO_4-P sorption has a broad pH plateau, with declines seen below pH 4 and above pH 8. The decline below pH 4 is due to build-up of the uncharged H_3PO_4, while the decline above pH 8, where HPO_4^{2-} predominates, may be due to a combination of increasing negative charge on the biochar surface and increasing OH^- ion concentration, both of which can compete with phosphate for interaction with excess pDADMAC charges. For 20% Mg softwood biochar, sorption is flat from pH 5.4 to 9.3, and begins to increase markedly above pH 9.3. A similar trend was observed with cypress-sawdust-derived Mg-doped biochar by Haddad et al. [56], who ascribed it to enhanced precipitation of Mg phosphate compounds at higher pH values [57]. By comparing the pH curves, it is clear that MgO-doped biochars have an advantage over pDADMAC-coated biochars at relatively high pH.

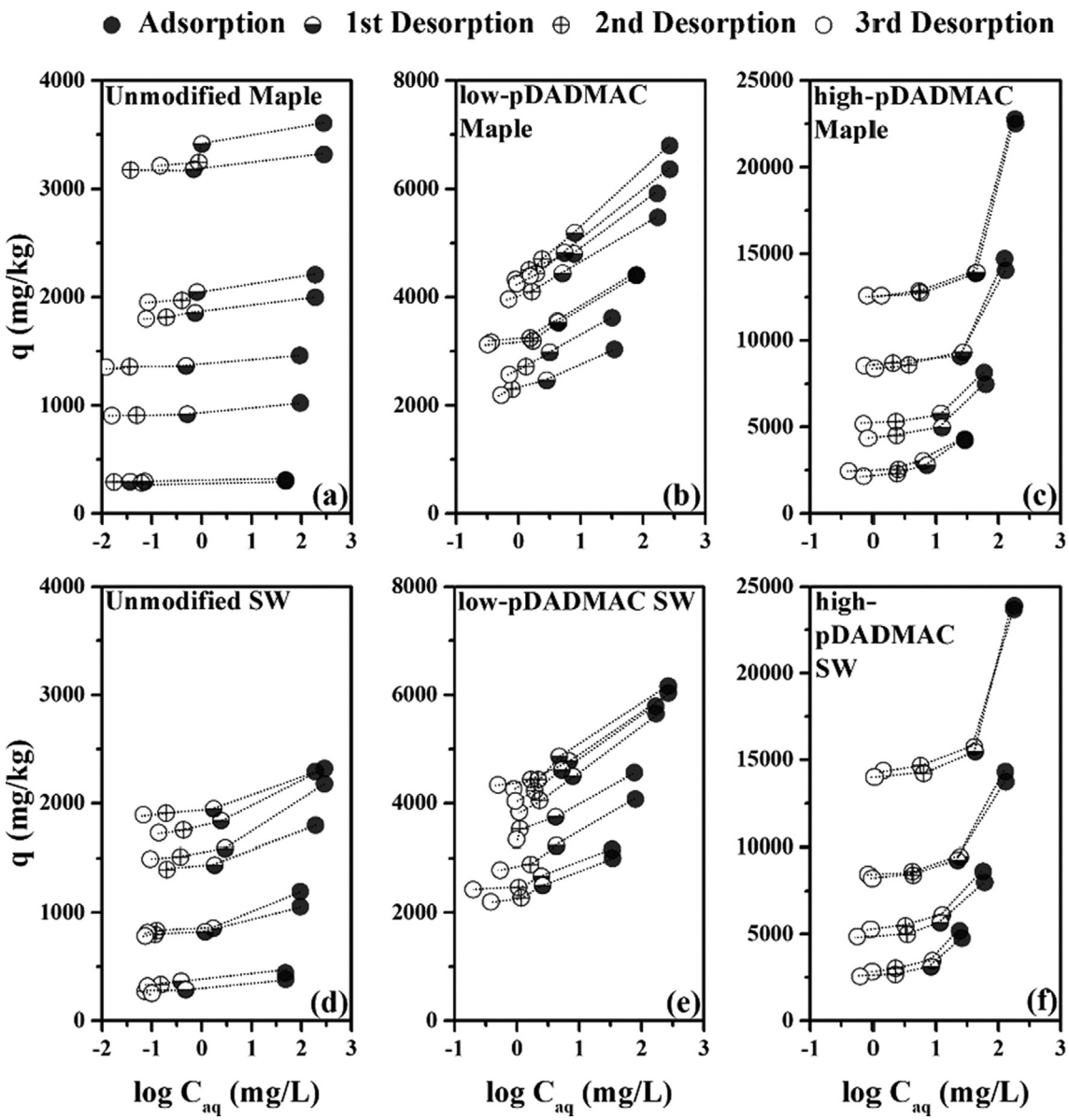

Fig. 6. Reversibility of phosphate sorption to pDADMAC-coated biochars. Sorption and desorption isotherms of biochars for (a) unmodified maple, (b) low-pDADMAC maple, (c) high-pDADMAC maple, (d) unmodified softwood (SW), (e) low-pDADMAC softwood, (f) high-pDADMAC softwood. C_{aq} is the liquid concentration and q the adsorption density. The lines connect the desorption data with their adsorption counterparts to guide the eye.

3.5. Mechanisms

Possible mechanisms of PO_4-P sorption include ion exchange, coordination with metals to form various species, and binding of phosphate ion pairs (e.g., along with K^+) by other forces, such as hydrogen bonding ([41] and references therein). In this study, the N1s XPS spectrum of pDADMAC-treated softwood biochar (Fig. 2a) is unchanged in position and intensity after sorption of phosphate, indicating that the quaternary N is electronically unperturbed. The phosphate peak in the P2p spectrum (Fig. 2b) appears at an energy consistent with its speciation as a mixture of $H_2PO_4^-$ and HPO_4^{2-} ions at the experimental pH for isotherms (Fig. 2f). The results show that phosphate binding by pDADMAC-treated softwood biochars is primarily by ion exchange, but we cannot rule out a small contribution from sorption of ion pairs. Another study showed that pDADMAC-coated clay mineral can bind $HAsO_4^{2-}$ and CrO_4^{2-} through electrostatic forces [38].

The mechanism by which pDADMAC is envisioned to function is shown in the Graphic Abstract. pDADMAC is first attached to the biochar surface by a combination of electrostatic forces with dissociated carboxyl and hydroxyl groups and van der Waals forces. As only a fraction of its quaternary ammonium groups will be neutralized by the surface negative charge, adsorption of pDADMAC will introduce excess positive charge to the particle. Moreover, because each polymer molecule has multiple points of attachment to the surface, its release back into solution is highly unfavorable under ordinary conditions due to entropy (i.e., all bonds must be cleaved before the molecule can diffuse back into bulk solution) [36]. PO_4-P (especially HPO_4^{2-}) is expected to favorably exchange with the native anion, Cl^-, since PO_4-P has a greater selectivity coefficient on quaternary ammonium anion exchange resins [52]. Hsieh and Pignatello [36] discovered that modification of activated carbons with pDADMAC could be a promising approach for in situ removal of hydrophobic compounds that are reactive towards anionic

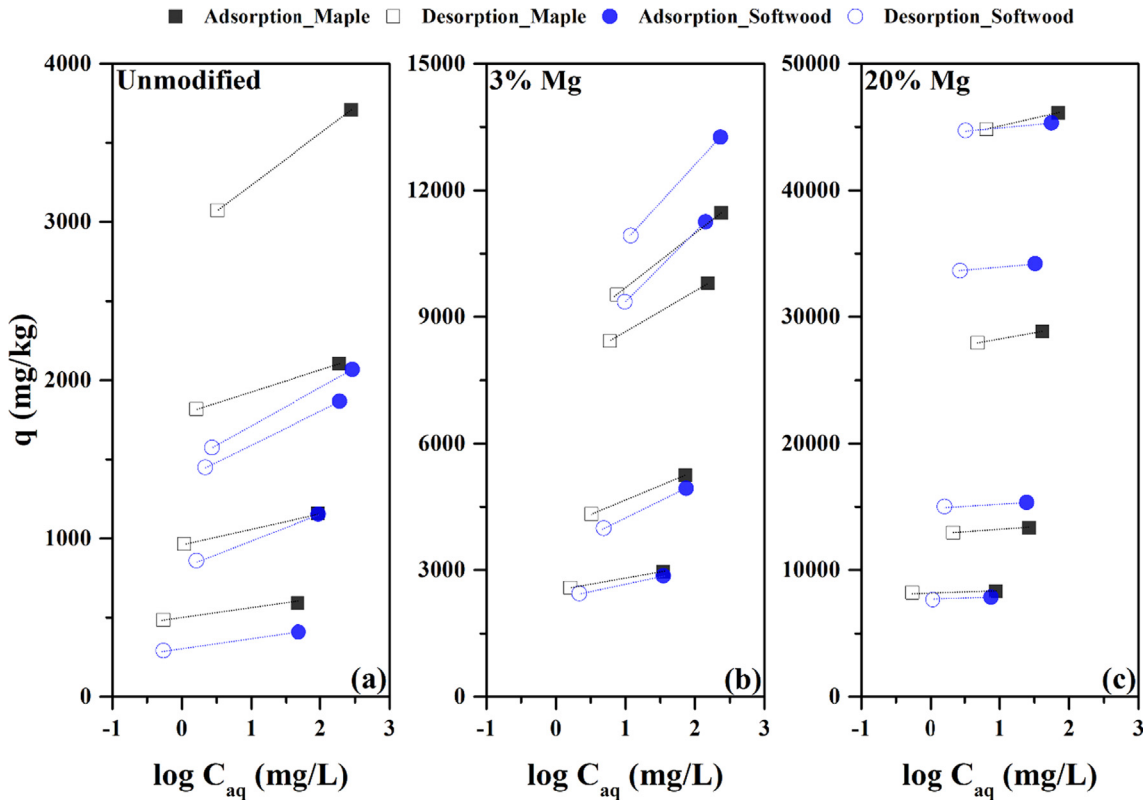

Fig. 7. Reversibility of PO_4-P sorption to Mg-doped biochars of (a) unmodified biochars; (b) 3% Mg-doped biochars; and (c) 20% Mg-doped biochars. The lines connect the desorption data with their adsorption counterparts to guide the eye.

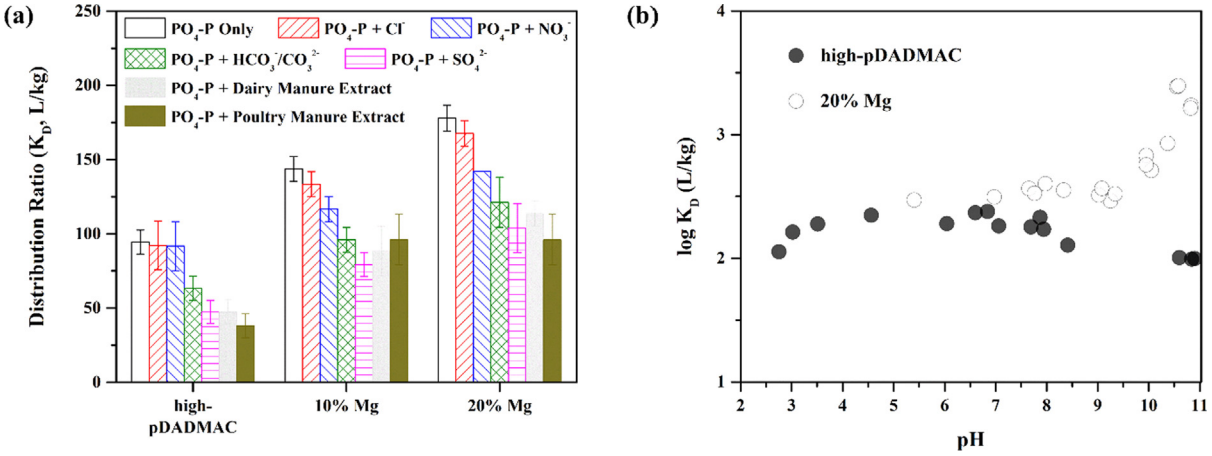

Fig. 8. Phosphate adsorption by modified softwood biochars (a) in the presence of anions and manure extracts and (b) as a function of pH. The distribution ratio $K_D = q/C_{aq}$. Conditions: initial P concentration = 1.02 mM, initial anion concentration = 2 mM, initial DOM concentration = 20.3 and 18.0 mg/L (dissolved organic carbon) for dairy and poultry manure extracts, respectively, initial pH = 8.0, temperature = 20 °C, solid loading = 0.5 g/L. Final pH is given in Fig. S2. The error bars indicate the range of duplicate experiments (n = 2). Experimental method for pH edge is seen in Text S3.

reagents (hydroxide in that case). They found that pDADMAC coating on the carbon at the level of 0.1 g/g, a) was essentially irreversible when pure water was used as the washing fluid; b) reversed the electrokinetic (zeta) potential negative to positive; and c) increased the AEC by almost 4-fold.

The XRD spectrum of Mg-doped softwood biochar as-prepared (Fig S5) shows only periclase (MgO), whereas the same biochar after phosphate sorption shows peaks for periclase and brucite ($Mg(OH)_2$). We attribute the appearance of brucite to hydrolysis of the top layer(s) of periclase after exposure to liquid water of the phosphate solution. We note that Xie et al. [53] found Mg $(OH)_2$ on MgO-doped diatomite after phosphate treatment. No XRD signals for magnesium phosphate minerals appear in the PO_4-P-treated sample. Likewise, Zhang et al. [42] found no XRD peaks for phosphate minerals after sorption of phosphate to a Mg-doped biochar prepared from biomass pre-soaked in $MgCl_2$ solution, although biochars from tomato plants allowed to take up Mg naturally showed XRD peaks corresponding to $MgHPO_4$ and $Mg(H_2PO_4)_2$ after phosphate sorption [41]. The Mg2p XPS spectrum of the as-prepared Mg-doped softwood biochar (Fig. 2c) shows a single peak consistent with MgO (50.8 eV [58,59]), which is shifted to higher energy after phosphate sorp-

tion. Deconvolution gives peaks for $MgHPO_4$ (51.6 eV [53,60]) and MgO (50.9 eV), along with a small peak for $Mg(OH)_2$ (49.6 eV [61]). The P2p XPS of the 20% Mg-doped biochar sorbed with phosphate (Fig. 2e) shows a peak at 134.5 eV which is 0.5 eV higher energy than the phosphate peak for pDADMAC-coated biochar (Fig. 2b). This is consistent either with coordination to Mg or a shift in phosphate speciation [62,63] due to the greater external pH (Fig. 2f).

The absence of crystalline phosphate minerals detected by XRD (Fig. S5), and the appearance of $MgHPO_4$ species in the Mg2p XPS, indicate that PO_4-P binding by the Mg-doped biochars is mainly due to formation of a Mg phosphate species on the $Mg(OH)_2$ surface layer. However, the results cannot clearly distinguish between individual phosphate ions tightly bound to surface-layer Mg that are spaced apart on the surface, or separate amorphous $MgHPO_4$ phases adhered to the surface. In other studies, binding of HPO_4^{2-} to $Mg(OH)_2$ was documented by Xie et al. [53] based on both XPS and solid state ^{31}P nuclear magnetic resonance spectroscopy. It is known that HPO_4^{2-} occupies one of the Mg octahedral coordination sites of $Mg(OH)_2$ [64,65]. Formation of surface complexes on Mg-doped biochars was detected with Fourier transform infrared spectroscopy in other works [66,67].

Water appears to induce desorption of phosphate more readily from pDADMAC-treated biochars compared to MgO-doped biochars (Fig. 6 vs Fig. 7). This can be explained by the differences in their respective sorption mechanism. The more facile desorption of phosphate from pDADMAC-treated biochars can be attributed to displacement of phosphate from ion exchange sites by water,

$$(\wr\cdots R_4N^+)(H_2PO_4^-) + H_2O \longrightarrow (\wr\cdots R_4N^+)(OH^-) + H_2PO_4^- + H^+ \quad (3)$$

or displacement of phosphate by adventitious ions that may be present in the water. Displacement of phosphate from Mg-doped biochars by water, however, is likely to be much more difficult because the mechanism of phosphate binding is primarily coordination to the surface metal ions. In both pDADMAC-treated and Mg-doped cases, it is also possibly to explain the partial reversibility by displacement of loosely-bound (K^+) phosphate ion pairs.

4. Conclusions

This study investigated PO_4-P sorption to and desorption from modified biochars in the presence or absence of competing anions or poultry/dairy manure extracts. Encouraging results for enhanced PO_4-P sorption are found by biochars coated with a quaternary ammonium polymer, pDADMAC; that is, the sorption densities are two-order-of-magnitude higher than the unmodified ones at environmental concentrations. Adsorption to the pDADMAC-coated biochars are of comparable magnitude to that of Mg-doped biochars on the basis of coating content. The pDADMAC-coated biochars are thus potentially suitable for removing phosphate from animal wastes or waste waters. In addition, sorption may be more reversible for the pDADMAC-coated biochars than the Mg-doped biochars, suggesting an advantage of the former for the purpose of re-use as a fertilizer. In regard to subsequent fertilizer value, it has been noted that metal-bound PO_4-P has low bioaccessibility due to the strength of the chemical bonds [68,69]. Additional work will be needed to determine whether phosphate is more bioaccessible in the ion-paired state when sorbed by the polymer-coated biochars, compared to the metal-bound state in the Mg-doped biochars. As implied by this study, strategically using carbonate or sulphate to desorb surface-attached phosphate may provide opportunities for phosphate recycling and/or modified biochar renewal in certain applications.

CRediT authorship contribution statement

Zhengyang Wang: Methodology, Investigation, Writing - original draft. **Santanu Bakshi:** Methodology, Investigation, Writing - original draft, Visualization. **Chongyang Li:** Investigation, Writing - review & editing. **Sanjai J. Parikh:** Conceptualization, Writing - review & editing, Supervision, Project administration, Funding acquisition. **Hsin-Se Hsieh:** Investigation, Writing - review & editing. **Joseph J. Pignatello:** Conceptualization, Writing - original draft, Visualization, Supervision, Project administration, Funding acquisition.

Declaration of Competing Interest

The authors declare that they have no known competing financial interests or personal relationships that could have appeared to influence the work reported in this paper.

Acknowledgements

This work was supported by a grant from the U.S. Department of Agriculture (USDA) National Institute of Food and Agriculture (NIFA) (Award# 2017-67019-26334). Additional support from USDA-NIFA Hatch Formula Funding and multistate regional project W-3045 is acknowledged. The authors thank Mr. Craig Musante at the Connecticut Agricultural Experiment Station for his assistance with ICP-OES, and Drs. Min Li and Jim Eckert at Yale University for their assistance with XPS/XRD/SEM and WDS analyses, respectively.

Appendix A. Supplementary data

Supplementary data to this article can be found online at https://doi.org/10.1016/j.jcis.2020.06.054.

References

[1] J. Manuel, Nutrient pollution: a persistent threat to waterways, Environ. Health Perspect. 122 (11) (2014) A304–A309.
[2] M.F. Chislock, E. Doster, R.A. Zitomer, A.E. Wilson, Eutrophication: causes, consequences, and controls in aquatic ecosystems, Nat. Educ. Knowledge 4 (4) (2013) 10.
[3] P.S. Kumar, L. Korving, M.C.M. van Loosdrecht, G.-J. Witkamp, Adsorption as a technology to achieve ultra-low concentrations of phosphate: research gaps and economic analysis, Water Res. X 4 (2019) 100029.
[4] A.T.W.M. Hendriks, J.G. Langeveld, Rethinking wastewater treatment plant effluent standards: nutrient reduction or nutrient control?, Environ. Sci. Technol. 51 (9) (2017) 4735–4737.
[5] S. Edmundson, M. Huesemann, R. Kruk, T. Lemmon, J. Billing, A. Schmidt, D. Anderson, Phosphorus and nitrogen recycle following algal bio-crude production via continuous hydrothermal liquefaction, Algal Res. 26 (2017) 415–421.
[6] E.D. Roy, Phosphorus recovery and recycling with ecological engineering: a review, Ecol. Eng. 98 (2017) 213–227.
[7] A.A. Szogi, M.B. Vanotti, K.S. Ro, Methods for treatment of animal manures to reduce nutrient pollution prior to soil application, Curr. Pollut. Rep. 1 (1) (2015) 47–56.
[8] J. Lehmann, S. Joseph, Biochar for Environmental Management: Science, Technology and Implementation, Routledge, New York, NY, 2015.
[9] D. Woolf, J.E. Amonette, F.A. Street-Perrott, J. Lehmann, S. Joseph, Sustainable biochar to mitigate global climate change, Nat. Commun. 1 (2010) 56.
[10] C.J. Atkinson, J.D. Fitzgerald, N.A. Hipps, Potential mechanisms for achieving agricultural benefits from biochar application to temperate soils: a review, Plant Soil 337 (1–2) (2010) 1–18.
[11] D.A. Laird, The charcoal vision: a Win–Win–Win scenario for simultaneously producing bioenergy, permanently sequestering carbon, while improving soil and water quality, Agron. J. 100 (2008) 178–181.
[12] A.S. Basso, F.E. Miguez, D.A. Laird, R. Horton, M. Westgate, Assessing potential of biochar for increasing water-holding capacity of sandy soils, GCB Bioenergy 5 (2) (2013) 132–143.
[13] D. Mohan, A. Sarswat, Y.S. Ok, C.U. Pittman, Organic and inorganic contaminants removal from water with biochar, a renewable, low cost and sustainable adsorbent – a critical review, Bioresour. Technol. 160 (2014) 191–202.

[14] J. Das, B.S. Patra, N. Baliarsingh, K.M. Parida, Adsorption of phosphate by layered double hydroxides in aqueous solutions, Appl. Clay Sci. 32 (3) (2006) 252–260.
[15] M.I. Inyang, B. Gao, Y. Yao, Y. Xue, A. Zimmerman, A. Mosa, P. Pullammanappallil, Y.S. Ok, X. Cao, A review of biochar as a low-cost adsorbent for aqueous heavy metal removal, Crit. Rev. Env. Sci. Technol. 46 (4) (2016) 406–433.
[16] M. Uchimiya, D.I. Bannon, Solubility of lead and copper in biochar-amended small arms range soils: influence of soil organic carbon and pH, J. Agric. Food Chem. 61 (32) (2013) 7679–7688.
[17] S. Bakshi, C. Banik, S.J. Rathke, D.A. Laird, Arsenic sorption on zero-valent iron-biochar complexes, Water Res. 137 (2018) 153–163.
[18] J.-H. Park, J.J. Wang, S.-H. Kim, S.-W. Kang, C.Y. Jeong, J.-R. Jeon, K.H. Park, J.-S. Cho, R.D. Delaune, D.-C. Seo, Cadmium adsorption characteristics of biochars derived using various pine tree residues and pyrolysis temperatures, J. Colloid Interface Sci. 553 (2019) 298–307.
[19] O. Paunovic, S. Pap, S. Maletic, M.A. Taggart, N. Boskovic, M. Turk Sekulic, Ionisable emerging pharmaceutical adsorption onto microwave functionalised biochar derived from novel lignocellulosic waste biomass, J. Colloid Interface Sci. 547 (2019) 350–360.
[20] A. Mukherjee, R. Lal, Biochar impacts on soil physical properties and greenhouse gas emissions, Agronomy 3 (2) (2013).
[21] K.A. Spokas, Impact of biochar field aging on laboratory greenhouse gas production potentials, GCB Bioenergy 5 (2) (2013) 165–176.
[22] Y. Yao, B. Gao, M. Zhang, M. Inyang, A.R. Zimmerman, Effect of biochar amendment on sorption and leaching of nitrate, ammonium, and phosphate in a sandy soil, Chemosphere 89 (11) (2012) 1467–1471.
[23] M.P. Sika, A.G. Hardie, Effect of pine wood biochar on ammonium nitrate leaching and availability in a South African sandy soil, Eur. J. Soil Sci. 65 (1) (2014) 113–119.
[24] M. Lawrinenko, D.A. Laird, Anion exchange capacity of biochar, Green Chem. 17 (9) (2015) 4628–4636.
[25] Q.-Z. Zhang, X.-H. Wang, Z.-L. Du, X.-R. Liu, Y.-D. Wang, Impact of biochar on nitrate accumulation in an alkaline soil, Soil Res. 51 (6) (2013) 521–528.
[26] O.A. Knowles, B.H. Robinson, A. Contangelo, L. Clucas, Biochar for the mitigation of nitrate leaching from soil amended with biosolids, Sci. Total Environ. 409 (17) (2011) 3206–3210.
[27] D. Laird, P. Fleming, B. Wang, R. Horton, D. Karlen, Biochar impact on nutrient leaching from a Midwestern agricultural soil, Geoderma 158 (3–4) (2010) 436–442.
[28] C.I. Kammann, H.-P. Schmidt, N. Messerschmidt, S. Linsel, D. Steffens, C. Müller, H.-W. Koyro, P. Conte, S. Joseph, Plant growth improvement mediated by nitrate capture in co-composted biochar, Sci. Rep. 5 (1) (2015) 11080.
[29] T. Clough, L. Condron, C. Kammann, C. Müller, A review of biochar and soil nitrogen dynamics, Agronomy 3 (2) (2013) 275–293.
[30] B. Glaser, J. Lehmann, W. Zech, Ameliorating physical and chemical properties of highly weathered soils in the tropics with charcoal – a review, Biol. Fertility Soils 35 (4) (2002) 219–230.
[31] J. Lehmann, J. Pereira da Silva, C. Steiner, T. Nehls, W. Zech, B. Glaser, et al., Nutrient availability and leaching in an archaeological Anthrosol and a Ferralsol of the Central Amazon basin: fertilizer, manure and charcoal amendments, Plant Soil 249 (2) (2003) 343–357.
[32] S. Jeffery, F.G.A. Verheijen, M. van der Velde, A.C. Bastos, A quantitative review of the effects of biochar application to soils on crop productivity using meta-analysis, Agr Ecosyst Environ 144 (1) (2011) 175–187.
[33] D. Laird, N. Rogovska, Biochar effects on nutrient leaching, in: J. Lehmann, S. Joseph (Eds.), Biochar for Environmental Management: Science, Technology and Implementation, Routledge Taylor & Francis Group, London; New York, 2015.
[34] Y. Cao, Y. Gao, Y. Qi, J. Li, Biochar-enhanced composts reduce the potential leaching of nutrients and heavy metals and suppress plant-parasitic nematodes in excessively fertilized cucumber soils, Environ. Sci. Pollut. Res. 25 (8) (2018) 7589–7599.
[35] R. Chintala, T.E. Schumacher, L.M. McDonald, D.E. Clay, D.D. Malo, S.K. Papiernik, S.A. Clay, J.L. Julson, Phosphorus sorption and availability from biochars and soil/biochar mixtures, Clean (Weinh) 42 (5) (2014) 626–634.
[36] H.-S. Hsieh, J.J. Pignatello, Modified carbons for enhanced nucleophilic substitution reactions of adsorbed methyl bromide, Appl. Catal. B 233 (2018) 281–288.
[37] G.E. Jackson, R.D. Letterman, Granular media filtration in water and wastewater treatment: Part 2, CRC Crit. Rev. Environ. Control 11 (1) (1980) 1–36.
[38] J.R. Ray, I.A. Shabtai, M. Teixidó, Y.G. Mishael, D.L. Sedlak, Polymer-clay composite geomedia for sorptive removal of trace organic compounds and metals in urban stormwater, Water Res. 157 (2019) 454–462.
[39] L. Paltrinieri, K. Remmen, B. Müller, L. Chu, J. Köser, T. Wintgens, M. Wessling, L.C.P.M. de Smet, E.J.R. Sudhölter, Improved phosphoric acid recovery from sewage sludge ash using layer-by-layer modified membranes, J. Membr. Sci. 587 (2019) 117162.
[40] B.E. Rittmann, B. Mayer, P. Westerhoff, M. Edwards, Capturing the lost phosphorus, Chemosphere 84 (6) (2011) 846–853.
[41] Y. Yao, B. Gao, J. Chen, L. Yang, Engineered biochar reclaiming phosphate from aqueous solutions: mechanisms and potential application as a slow-release fertilizer, Environ. Sci. Technol. 47 (15) (2013) 8700–8708.
[42] M. Zhang, B. Gao, Y. Yao, Y. Xue, M. Inyang, Synthesis of porous MgO-biochar nanocomposites for removal of phosphate and nitrate from aqueous solutions, Chem. Eng. J. 210 (2012) 26–32.
[43] R.B. Fidel, D.A. Laird, M.L. Thompson, Evaluation of modified boehm titration methods for use with biochars, J. Environ. Qual. 42 (6) (2013) 1771–1778.
[44] T.B. Scott, G.C. Allen, P.J. Heard, M.G. Randell, Reduction of U(VI) to U(IV) on the surface of magnetite, Geochim. Cosmochim. Acta 69 (24) (2005) 5639–5646.
[45] E.W. Rice, R.B. Baird, A.D. Eaton, L.S. Clesceri, Standard Methods for the Examination of Water and Wastewater, APHA, AWWA, WEF, Washington, D.C., 2012.
[46] J. Murphy, J.P. Riley, A modified single solution method for the determination of phosphate in natural waters, Anal. Chim. Acta 27 (1962) 31–36.
[47] J.E. Harwood, R.A. van Steenderen, A.L. Kühn, A rapid method for orthophosphate analysis at high concentrations in water, Water Res. 3 (6) (1969) 417–423.
[48] S. Chen, H. Tanaka, Surface analysis of paper containing polymer additives by X-ray photoelectron spectroscopy I: application to paper containing dry strength additives, J. Wood Sci. 44 (4) (1998) 303–309.
[49] L. Pei, C.A. Lucy, Insight into the stability of poly (diallydimethylammoniumchloride) and polybrene poly cationic coatings in capillary electrophoresis, J. Chromatogr. A 1365 (2014) 226–233.
[50] Z.J. Yu, E.T. Kang, K.G. Neoh, Electroless plating of copper on polyimide films modified by surface grafting of tertiary and quaternary amines polymers, Polymer 43 (15) (2002) 4137–4146.
[51] N.A. Oladoja, S. Chen, J.E. Drewes, B. Helmreich, Characterization of granular matrix supported nano magnesium oxide as an adsorbent for defluoridation of groundwater, Chem. Eng. J. 281 (2015) 632–643.
[52] H.P. Gregor, J. Belle, R.A. Marcus, Studies on ion-exchange resins. XIII. Selectivity coefficients of quaternary base anion-exchange resins toward univalent anions, J. Am. Chem. Soc. 77 (10) (1955) 2713–2719.
[53] F. Xie, F. Wu, G. Liu, Y. Mu, C. Feng, H. Wang, J.P. Giesy, Removal of phosphate from eutrophic lakes through adsorption by in situ formation of magnesium hydroxide from diatomite, Environ. Sci. Technol. 48 (1) (2014) 582–590.
[54] L.R. Cooperband, L.W. Good, Biogenic phosphate minerals in manure: implications for phosphorus loss to surface waters, Environ. Sci. Technol. 36 (23) (2002) 5075–5082.
[55] E. Weyers, D.G. Strawn, D. Peak, L.L. Baker, Inhibition of phosphorus sorption on calcite by dairy manure-sourced DOC, Chemosphere 184 (2017) 99–105.
[56] K. Haddad, S. Jellali, M. Jeguirim, A. Ben Hassen Trabelsi, L. Limousy, Investigations on phosphorus recovery from aqueous solutions by biochars derived from magnesium-pretreated cypress sawdust, J. Environ. Manage. 216 (2018) 305–314.
[57] M. Darn Simon, R. Sodi, R. Ranganath Lakshminarayan, B. Roberts Norman, R. Duffield John, Experimental and computer modelling speciation studies of the effect of pH and phosphate on the precipitation of calcium and magnesium salts in urine, Clin. Chem. Lab. Med. 44 (2) (2006) 185.
[58] Y. Inoue, I. Yasumori, Catalysis by alkaline earth metal oxides. III. X-ray photoelectron spectroscopic study of catalytically active MgO, CaO, and BaO surfaces, Bull. Chem. Soc. Jpn. 54 (5) (1981) 1505–1510.
[59] R. Hoogewijs, L. Fiermans, J. Vennik, Electronic relaxation processes in the KLL auger spectra of the free magnesium atom, solid magnesium and MgO, J. Electron Spectrosc. Relat. Phenom. 11 (2) (1977) 171–183.
[60] X. Zhu, Y. Liu, F. Qian, H. Shang, X. Wei, S. Zhang, J. Chen, Z.J. Ren, Carbon transmission of CO_2 activated nano-MgO carbon composites enhances phosphate immobilization, J. Mater. Chem. A 6 (8) (2018) 3705–3713.
[61] K.Z. Chong, T.S. Shih, Conversion-coating treatment for magnesium alloys by a permanganate–phosphate solution, Mater. Chem. Phys. 80 (1) (2003) 191–200.
[62] H. Yan, Q. Chen, J. Liu, Y. Feng, K. Shih, Phosphorus recovery through adsorption by layered double hydroxide nano-composites and transfer into a struvite-like fertilizer, Water Res. 145 (2018) 721–730.
[63] Z. Ren, X. Xu, X. Wang, B. Gao, Q. Yue, W. Song, L. Zhang, H. Wang, FTIR, Raman, and XPS analysis during phosphate, nitrate and Cr(VI) removal by amine cross-linking biosorbent, J. Colloid Interface Sci. 468 (2016) 313–323.
[64] J.W. Yun, T. Tanase, S.J. Lippard, Carboxylate- and phosphate ester-bridged dimagnesium(II), dizinc(II), and dicalcium(II) complexes. Models for intermediates in biological phosphate ester hydrolysis, Inorg. Chem. 35 (26) (1996) 7590–7600.
[65] F. Brunet, T. Schaller, Protons in the magnesium phosphates phosphoellenbergerite and holtedahlite; an IR and NMR study, Am. Mineral. 81 (3–4) (1996) 385–394.
[66] D. Jiang, B. Chu, Y. Amano, M. Machida, Removal and recovery of phosphate from water by Mg-laden biochar: batch and column studies, Colloids Surf. Physicochem. Eng. Aspects 558 (2018) 429–437.
[67] M. Yi, Y. Chen, Enhanced phosphate adsorption on Ca-Mg-loaded biochar derived from tobacco stems, Water Sci. Technol. 78 (11) (2019) 2427–2436.
[68] J.K. Syers, A.E. Johnston, D. Curtin, Efficiency of soil and fertilizer phosphorus use, FAO Fertilizer Plant Nutrit. Bull. 18 (108) (2008).
[69] J.J. Weeks, G.M. Hettiarachchi, A review of the latest in phosphorus fertilizer technology: possibilities and pragmatism, J. Environ. Qual. 48 (5) (2019) 1300–1313.